Phase-Change Materials in Optically Triggered Microactuators

Johannes A. Kalb, Qiang Guo, Xiaoqiang Zhang, Yi Li, Chornghaur Sow, and Carl V. Thompson

***Abstract*—Phase-change materials have been extensively used for optical data storage in commercial rewritable compact disks and digital video disks. These materials are also widely considered for next-generation phase-change random access memories to replace current Flash memories. We suggest a different application of phase-change materials in optically triggered microactuators. The suggested device consists of a thin film of a phase-change material deposited on a microfabricated cantilever. A laser-induced phase transformation in the film initiates a cantilever deflection since the transformation is accompanied by a large density change. We analyze quantitative criteria for material selection and optimization of device dimensions for the largest possible actuation angles and deflections. The resulting analytical model is both verified numerically and applied experimentally. Furthermore, we show that these cantilevers offer a convenient way to measure film stresses and film strains associated with laser-induced phase transformations. [2007-0276]**

***Index Terms*—Actuators, laser annealing, stress measurement, tellurium alloys.**

I. Introduction

IN REWRITABLE compact disks (CD-RWs) and digital video disks (DVD-RW and DVD-RAM), a thin film of a phase-change material (usually an SbTe alloy) is locally and reversibly switched between the amorphous and crystalline states, using pulsed laser heating and fast cooling to amorphize the material and using laser heating to crystallize the material. The amorphous and crystalline states can be optically distinguished due to their pronounced difference in reflectivity [1]–[3]. Recently, phase-change materials have also been employed in industrial test devices for electronic nonvolatile data storage [2], [4]–[6]. In these so-called *phase-change random access memories* (PCRAM, PRAM, or PCM), electrical power provides the heat that is necessary for the transformation between the amorphous and crystalline states, which can be distinguished subsequently by their pronounced difference in electrical conductivity [7]–[9]. Due to their higher speed, larger number of write–erase cycles, and better scaling characteristics, PCRAMs show high potential to replace current Flash memories, i.e., to serve as the next generation of nonvolatile memories for portable multimedia devices [2], [4]–[6].

Phase-change materials are characterized by a large density or volume difference between the amorphous and crystalline phases, [7], [9]–[11] on the order of 6%–9%, which is related to the large optical contrast between the two phases [12], [13]. However, such a large volume change can induce a large film stress in the gigapascal regime [10]. Wafer curvature (WC) measurements during furnace heating of amorphous SbTe films deposited on Si wafers have revealed that a substantial part of this stress is inelastically relaxed during crystallization [10]. This effect is undesirable in data storage since it leads to material fatigue and therefore limits the maximum number of write–erase cycles. It is therefore important to develop materials and methods for which volume changes and their effects are minimized. This could enable phase-change media to compete with those data-storage media that can sustain far more write–erase cycles than Flash memories, such as dynamic RAMs and magnetic hard drives.

Stresses or strains induced *locally* by laser-induced crystallization have not yet been systematically investigated for SbTe alloys. Therefore, we present a study of laser crystallization of amorphous phase-change films deposited on rectangular microfabricated cantilever beams [Fig. 1(a) and (b)]. The associated volume contraction upon crystallization induces cantilever bending [Fig. 1(c)] that provides a measure of the stress or strain in the film. In addition, such a system could serve as a microactuator in a switch or for a movable mirror. Since the cantilever movement is controlled *externally* without the need for electronic components near the cantilever, *arrays* of these devices could be manufactured on a wide range of substrates and at potentially low cost. Large-area optically triggered micromirror arrays could, for example, be manufactured on expansive substrates, and images could be written and erased with external laser sources. The actuation could even be reversible if subsequent amorphization could counterbalance the crystallization-induced cantilever movement. However, this paper only focuses on crystallization, i.e., nonreversible actuation. It should be noted that even though many amorphous films can be laser crystallized, phase-change materials are particularly suitable for this application due to their large volume change between the two phases, which would induce high actuation

Manuscript received November 21, 2007; revised April 15, 2008. First published August 15, 2008; current version published October 1, 2008. This work was supported by the Singapore-MIT Alliance. The work of J. A. Kalb was supported in part by the Alexander von Humboldt Foundation. Subject Editor H. Zappe.

J. A. Kalb is with the Department of Materials Science and Engineering, Massachusetts Institute of Technology, Cambridge, MA 02139-4307 USA (e-mail: joh.otm@kalb.eu).

Q. Guo and X. Zhang are with the Singapore–MIT Alliance, National University of Singapore, Singapore 117576.

Y. Li is with the Department of Materials Science and Engineering, National University of Singapore, Singapore 117574.

C. Sow is with the Department of Physics, Faculty of Science, National University of Singapore, Singapore 117542.

C. V. Thompson is with the Department of Materials Science and Engineering, Massachusetts Institute of Technology, Cambridge, MA 02139-4307 USA (e-mail: cthomp@mit.edu).

Color versions of one or more of the figures in this paper are available online at http://ieeexplore.ieee.org.

Digital Object Identifier 10.1109/JMEMS.2008.928708

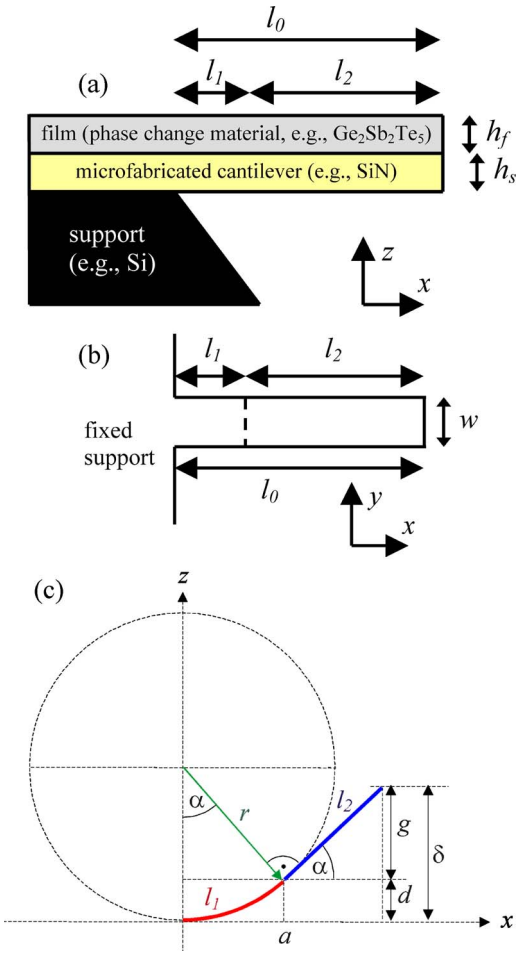

Fig. 1. (a) Schematic side view of a microfabricated cantilever of length l_0 with a fixed support on the left side. A thin film of an amorphous phase-change material has been deposited on the cantilever. The thicknesses of the cantilever and film are h_s and h_f, respectively, and are not drawn to scale. (b) Schematic top view of the cantilever in (a). The film is laser crystallized in the region $l_1 \times w \times h_f$ and remains amorphous in the region $l_2 \times w \times h_f$. The cantilever underneath does not undergo a phase transformation during this process. Due to the volume contraction in the region $l_1 \times w \times h_f$, the cantilever moves upward. (c) Schematic side view of the cantilever shown in (a) and (b) after laser crystallization. For clarity, the thickness of the structure is not indicated. All dashed lines and curves are guides to the eye. The crystallized region of length l_1 curves with a radius r. The remaining part of the cantilever that is still coated with an amorphous film is aligned as a tangent to the dashed circle at $x = a$. It is inclined by the actuation angle α toward the original horizontal cantilever position before laser crystallization. δ is the actuation height.

angles α's [Fig. 1(c)]. While minimum volume changes are desired for memory applications, maximum volume changes are desirable for actuation applications of phase-change materials. However, it should also be noted that materials with smaller volume changes could be used in applications for which smaller actuation angles are acceptable.

II. Cantilever Design and Optimization

Analytical and numerical strain analyses of the bilayer system in Fig. 1 were performed in order to understand for which conditions the highest possible angle α and the highest possible deflection δ can be obtained for a given volume change and for given dimensions l_1 and l_2 [(Fig. 1(c)]. This facilitates both stress and strain measurements and allows the design of optimized optically triggered actuators. The analysis is initially performed in a general way, i.e., no specific material parameters are assumed. An ideal thickness ratio $h = h_f/h_s$ of film and cantilever is calculated as a function of their elastic constants [Fig. 1(a)].

A. Analytical Analysis

Using Fig. 1(c), the following can be derived geometrically:

$$\alpha = \frac{1}{r} \cdot l_1 \tag{1}$$

$$\delta = \underbrace{r \cdot (1 - \cos(\alpha))}_{d} + \underbrace{(l_0 - l_1) \cdot \sin(\alpha)}_{g} \tag{2a}$$

where $l_0 = l_1 + l_2$ is the length of the cantilever. The quantities d, g, r, α, and δ are shown in Fig. 1(c). Equations (1) and (2a) are exact for any angle α between 0° and 360°. For small angles, which typically occur in deflection experiments or actuation applications, $\sin(\alpha) \approx \alpha$ and $1 - \cos(\alpha) \approx \alpha^2/2$, so that (2a) simplifies to

$$\delta = \frac{1}{r} \cdot l_1 \cdot \left(l_0 - \frac{l_1}{2} \right). \tag{2b}$$

It is assumed in the following that each of the two layers in Fig. 1(a) is elastically isotropic so that an equibiaxial stress (or an equibiaxial strain) occurs in each layer as a result of the crystallization-induced volume change in the region $l_1 \times w \times h_f$. Edge effects (nonuniform stresses and strains close to the boundary of this region) are assumed to have no significant impact on the radius of curvature r of the region $l_1 \times w \times h_f$ (a numerical verification of this assumption follows in the next section). We analyze the problem for the general case that h_f does *not* need to be small compared with h_s. Therefore, both stress and strain in either layer vary linearly through the layer thickness [14], [15]. At the interface between the regions $l_1 \times w \times h_f$ and $l_0 \times w \times h_s$, a lateral (or in-plane) elastic mismatch strain ε_m and an associated lateral (or in-plane) elastic mismatch stress σ_m occur [14], [15] (note that for $h \ll 1$, ε_m and σ_m reduce to the in-plane biaxial *film* strain and the in-plane biaxial *film* stress, respectively, which are then essentially independent of thickness coordinate). The radius r [Fig. 1(c)] can then be calculated analytically from Stoney's equation, which, for arbitrary film thickness ratio $h = h_f/h_s$, has the general form [14], [15]

$$\frac{1}{r} = \frac{\varepsilon_m}{h_s} \cdot p(h, m). \tag{3}$$

ε_m is zero before the crystallization-induced volume change and is defined positive afterward. $p(h, m)$ is a function of the thickness ratio h and the biaxial elastic modulus ratio $m = M_f/M_s$, where $M_f = E_f/(1 - \nu_f)$ and $M_s = E_s/(1 - \nu_s)$ are the biaxial elastic moduli of the film and cantilever, respectively. E and ν are the Young's modulus and Poisson's ratio of the respective layer. $p(h, m)$ is given by [14], [15]

$$p(h, m) = \frac{6hm(1 + h)}{1 + 4hm + 6h^2m + 4h^3m + h^4m^2} \tag{4}$$

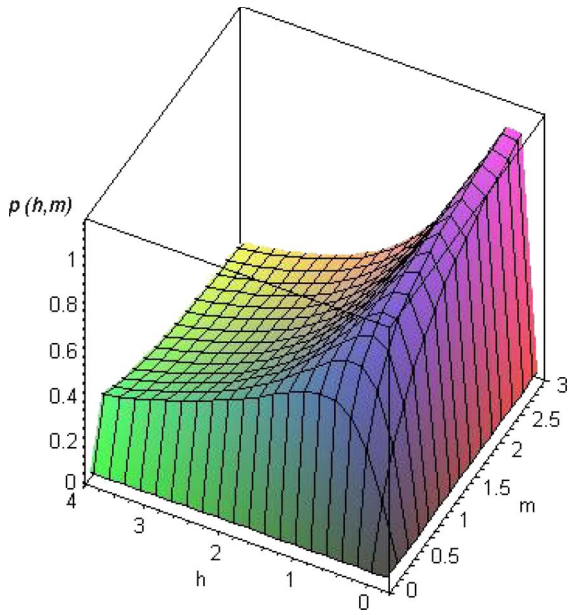

Fig. 2. Plot of (4). $h = h_f/h_s$ and $m = M_f/M_s$, where h_f and h_s are shown in Fig. 1. M_f and M_s are the biaxial elastic moduli of the film and cantilever, respectively. Since the actuator deflection α and the actuation height δ are proportional to the quantity $p(h, m)$ [(5) and (6)], a maximum value for $p(h, m)$ is desired.

and is shown in Fig. 2. Since (3) and (4) only depend on the modulus ratio, a replacement of the biaxial modulus $M = E/(1-\nu)$ by the plate modulus $M = E/(1-\nu^2)$ would not significantly affect the result as long as the Poisson ratio of film and cantilever are approximately equal. It should be noted that any stresses that relax *plastically* during or after the phase transformation do not contribute to the cantilever curvature and therefore do not enter (3). Therefore, $3 \cdot \varepsilon_m \leq |\Delta V/V|$, where $|\Delta V/V|$ is the crystallization-induced volume change of a hypothetically unconstrained amorphous material, which is around 6%–9% for phase-change materials [7], [9]–[11], [16]. The "=" sign in the aforementioned expression applies to a purely elastic phase transformation, whereas the "<" sign holds for a transformation that includes plastic stress relaxation. Therefore, for phase-change materials, ε_m should be on the order of 2%–3% (or 0.02–0.03) for a purely elastic transformation and smaller otherwise.

Substituting (3) into (1) and (2b) gives

$$\alpha = \frac{\varepsilon_m}{h_s} \cdot p(h,m) \cdot l_1 \tag{5}$$

$$\delta = \frac{\varepsilon_m}{h_s} \cdot p(h,m) \cdot l_1 \cdot \left(l_0 - \frac{l_1}{2}\right). \tag{6}$$

Therefore, for given parameters l_0, l_1, and ε_m, the following two design rules have to be followed in order to maximize α and δ and thereby to optimize the actuation magnitude.

1) h_s should be minimized.
2) $p(h, m)$ should be maximized.

While rule 1) appears intuitively clear, rule 2) implies that an ideal value $h_{\text{ideal}}(m)$ may exist for a given modulus ratio m. h_{ideal} was found by differentiating (4) with respect to h (while treating m as a constant), equating the result to zero, and then solving for h. Fig. 3 shows the result. A simple example is the case in which the film and cantilever have the same biaxial modulus, i.e., $m = 1$. Fig. 3 shows that $h_{\text{ideal}}(m = 1) = 1/2$, i.e., the film should be half as thick as the cantilever for ideal deflection performance. Inserting $h_{\text{ideal}}(m)$ into (4) gives the maximum value $p_{\max}(m) := p(h_{\text{ideal}}(m), m)$ as a function of m (Fig. 4).

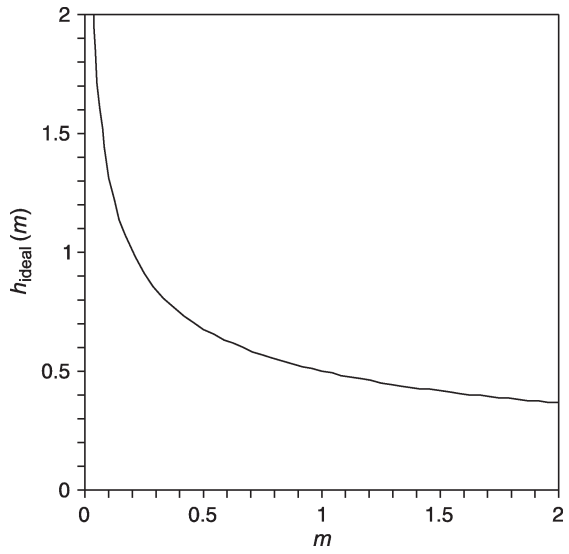

Fig. 3. Ideal ratio $h_{\text{ideal}}(m)$ of film thickness to cantilever thickness that results in maximum actuator deflection. $h_{\text{ideal}}(m)$ only depends on the biaxial modulus *ratio* of the bilayer, $m = M_f/M_s$. For example, if the film and cantilever have the same biaxial modulus, $h_{\text{ideal}}(m = 1) = 1/2$.

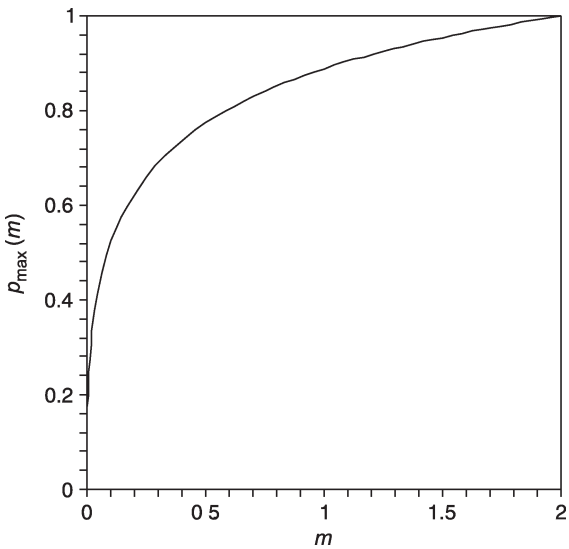

Fig. 4. Maximum value in (4), $p_{\max}(m) := p(h_{\text{ideal}}(m), m)$, as a function of biaxial modulus ratio $m = m_f/m_s$. $h_{\text{ideal}}(m)$ is the ideal thickness ratio from Fig. 3 that results in maximum actuator deflection.

We now compare the performance of Si and SiN, which are technologically important cantilever materials. $Ge_2Sb_2Te_5$ is chosen as the phase-change film since this material is well understood and most widely used in phase-change recording [1], [2], [4]. The biaxial modulus of $Ge_2Sb_2Te_5$ films is $M_f = 45.2 \pm 8.2$ GPa [17]. (100) Si has a well-established biaxial modulus [18] of $M_s^{(\text{Si})} = 180.5$ GPa, which, in combination

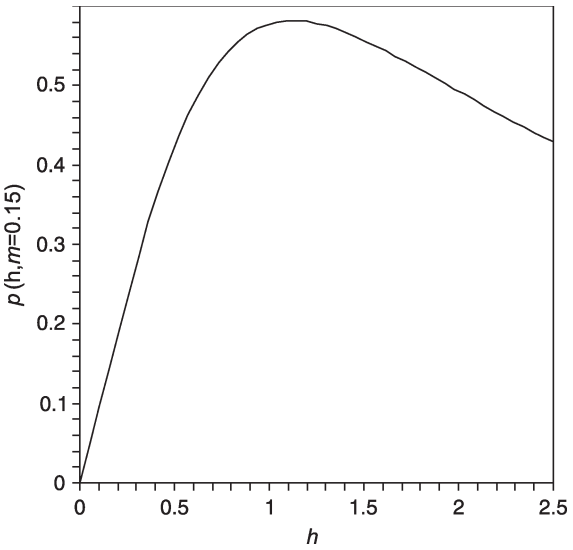

Fig. 5. Section through the surface in Fig. 2 for a biaxial modulus ratio $m = 0.15$, which corresponds to a bilayer of $Ge_2Sb_2Te_5$ and SiN. The quantity $p(h, m = 0.15)$, which is proportional to the actuation angle α and the actuation height δ [(5) and (6)], is maximal for the value $h_{\text{ideal}} = 1.12$.

with the $Ge_2Sb_2Te_5$ film, gives $m^{(\text{Si})} = M_f/M_s^{(\text{Si})} = 0.25 \pm 0.05$. It follows that $h_{\text{ideal}}^{(\text{Si})} = 0.91 \pm 0.06$ (Fig. 3) and $p_{\max}^{(\text{Si})} = 0.66 \pm 0.03$ (Fig. 4). Therefore, the $Ge_2Sb_2Te_5$ film thickness should be about 91% of the Si cantilever thickness. Young's modulus $E_s^{(\text{SiN})}$ for SiN films can vary substantially between roughly 190 and 270 GPa [19], [20]. We take $E_s^{(\text{SiN})} = 219 \pm 25$ GPa, which we determined for the SiN cantilevers used for the experiments to be described in Section III. This value was measured by cantilever bending using an atomic force microscope (AFM, Digital Instruments 3100) in contact mode [21]. Poisson's ratio for the SiN cantilever is assumed to be $\nu_s^{(\text{SiN})} = 0.27$, as suggested by literature data [19]. This gives $m^{(\text{SiN})} = M_f/M_s^{(\text{SiN})} = 0.15 \pm 0.03$, $h_{\text{ideal}}^{(\text{SiN})} = 1.12 \pm 0.09$ (Fig. 3), and $p_{\max}^{(\text{SiN})} = 0.58 \pm 0.04$ (Fig. 4). Hence, the $Ge_2Sb_2Te_5$ film should be about 12% thicker than the SiN cantilever. Therefore, for the same lateral dimensions, Si cantilevers can exhibit an actuation angle α and a deflection height δ that is higher by about $0.66/0.58 = 1.14$ or 14% compared to SiN cantilevers.

Fig. 5 shows a section through the surface in Fig. 2, for $m^{(\text{SiN})} = 0.15$. The curve is characterized by a relatively broad maximum at $h_{\text{ideal}}^{(\text{SiN})} = 1.12$, which indicates that even moderate deviations from the suggested ideal thickness ratio $h_{\text{ideal}}^{(\text{SiN})}$ during manufacturing would still yield almost the same value $p_{\max}^{(\text{SiN})} = 0.58$ and, therefore, the same ideal actuation angle α or actuation height δ. This is of benefit for potential applications that require tight performance variations between devices that are manufactured from different film deposition runs.

As an example for a $Ge_2Sb_2Te_5$ film on a SiN cantilever, we take $\varepsilon_m = 0.01$ or 1% (which would imply that roughly one-third to one-half of the induced stress upon crystallization relaxes plastically), $h_s = 200$ nm (as a consequence, $h_f = 1.12 \cdot 200$ nm $= 224$ nm as outlined earlier), $p_{\max}^{(\text{SiN})} = 0.58$, $l_1 = 3$ μm, and $l_0 = 13$ μm. Equations (5) and (6) then give $\alpha = 5^\circ$ and $\delta = 1$ μm.

B. Numerical Analysis

To verify the analytical model, a finite-element analysis (FEA, Abaqus 6.5) was performed with the cantilever shown in Fig. 1. The FEA serves as a benchmark for the analytical model described before. Dimensions of $l_0 = 50$ μm and $h_s = h_f = 200$ nm were chosen, which are close to the dimensions used in the experiments (Section III-D). Two cases were simulated, one with $w = 2.5$ μm and one with $w = 5$ μm. Quadratic continuum (3-D solid) elements with reduced integration were used (full integration gave almost exactly the same result). These elements are suitable due to the 3-D nature of the problem (the cantilever is not thin compared to its width). Both film and cantilever were assumed to be elastically isotropic. The biaxial modulus and the Poisson ratio were chosen to be equal to the values for SiN and $Ge_2Sb_2Te_5$ mentioned in Section II-A. For $Ge_2Sb_2Te_5$, a Poisson ratio of $\nu = 0.3$ was assumed, a typical value for inorganic solids [19]. The *elastic part* of the crystallization-induced volume change was simulated by a hypothetical elastic and isotropic thermal contraction during a hypothetical temperature decrease: For simulation purposes, both effects are equivalent. A hypothetical linear thermal expansion coefficient of $\alpha_{\text{th}} = 10^{-5}/\text{K}$ was assigned to the region $l_1 \times w \times h_f$ (Fig. 1), whereas a zero thermal expansion coefficient was assigned to all other regions. A temperature decrease of $|\Delta T| = 1000$ K was then applied to the entire model, which resulted in a linear isotropic contraction of $|\varepsilon_m| = \alpha_{\text{th}} \cdot |\Delta T| = 10^{-2}$ or 1%. Since this analysis treats only the *elastic* contraction, this hypothetical process yields the same cantilever deflection as the crystallization-induced elastic volume decrease that induces the lateral elastic mismatch strain $\varepsilon_m = 10^{-2}$ discussed earlier (any inelastic stress relaxation was not simulated since only the elastic part induces a cantilever curvature). The size of the finite elements in the simulation was decreased until the calculated values for angle α and deflection δ reached saturation values (mesh convergence). During this process, a substantially denser mesh was used in the region where the phase transformation occurred. The smallest simulated element size was 25 nm. Several simulations were run to vary the length l_1 between 0.5 and 14 μm. The circles in Fig. 6 show the results for the 5-μm-wide beam (results for the 2.5-μm-wide beam are almost identical and therefore not shown). For comparison, the solid curves represent the analytical model from (5) and (6). The numerical and analytical analyses deviate by less than 10% for 0.5 $\mu\text{m} \leq l_1 \leq 2$ μm and by less than 5% for 2 $\mu\text{m} < l_1 \leq 14$ μm. This small deviation still holds if the biaxial modulus for SiN or $Ge_2Sb_2Te_5$ is increased or decreased by a factor of two from the values mentioned previously. Therefore, using the FEA as a benchmark, it can be concluded that edge effects (which are neglected in the analytical calculation) close to the clamped edge of the cantilever (rim of the region $l_1 \times w \times h_f$) influence the angle α and height δ [Fig. 1(c)] by only about 5%–10%. It should be noted that Sader [22] has derived analytical correction terms to Stoney's deflection value δ for *clamped* cantilevers. His treatment, however, is only valid if the film thickness is negligible compared with the cantilever thickness, which is not the case in this paper. A derivation of such correction terms for thick films is complex and beyond the

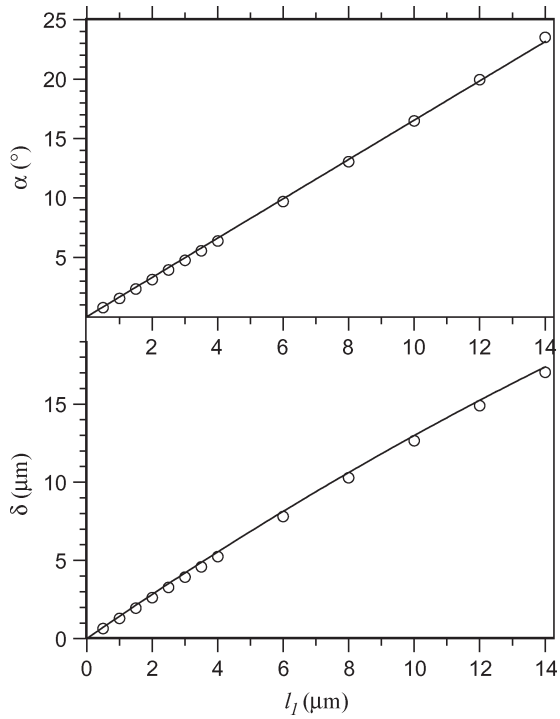

Fig. 6. (Circles) Finite-element simulation results compared with (solid lines) analytical calculations from (5) and (6) for cantilever deflection angles α's and heights δ's [cf. Fig. 1(c)]. Input parameters were $l_0 = 50$ μm, $h_s = h_f = 200$ nm, and $\varepsilon_m = 10^{-2}$. Material parameters were $E_s = 219 \pm 25$ GPa and $\nu_s = 0.27$ (SiN cantilever) and $M_f = (45.2 \pm 8.2)$ GPa and $\nu_f = 0.30$ ($Ge_2Sb_2Te_5$ film).

scope of this paper. Therefore, it has to be kept in mind that the uncertainty of the analytical model in Section II-A can be up to 5%–10%.

III. Experimental Application

A. SiN Cantilever Fabrication

Since Si cantilevers offer only a 14% better performance than SiN cantilevers, the latter were chosen for fabrication as they are both easier and less expensive to fabricate. Low-stress Si-rich SiN films were deposited on both sides of double-side-polished (100) Si wafers using chemical vapor deposition (CVD) at 775 °C, using a vertical thermal reactor (Silicon Valley Group, VTR 6000). The Si wafers were 675 ± 25 μm thick and had a diameter of 150 mm. The gas flow rates were 250-sccm dichlorosilane (H_2Cl_2Si) and 25-sccm ammonia (NH_3), and the pressure was 250 mtorr. The deposition rate was 3.1 nm/min. The film thickness and the refractive index were $h_s = 211 \pm 3$ nm and $n = 2.25 \pm 0.01$, respectively, as determined by ellipsometry (KLA-Tencor, Model UV1250SE). Previous wafer curvature (WC) studies [23] have shown that this gas recipe gives SiN films with an average tensile stress on the order of 125 MPa. h_s was chosen to be as small as practically possible in order to give a large actuator deflection. However, a SiN thickness below about 200 nm would have greatly increased [23] the risk of pin-hole formation during wet etching in potassium hydroxide (KOH; see hereafter).

Positive photoresist of 800-nm thickness was spin coated on the SiN film on the front side of the wafer. The resist was exposed by contact lithography (EV Group, Model EV620) with UV light using a mercury lamp through a photomask. The photomask contained cantilevers of various dimensions (both l_0 and w were varied between 2 and 100 μm). After developing the resist, the SiN on the front side was etched in a gas-phase process (LAM Research, Model 490B). The developed photoresist served as an etch mask. The gas flow rates were 190-sccm sulfur hexafluoride (SF_6) and 19-sccm oxygen (O_2), and the pressure was 300 mtorr. The time to etch through the entire SiN film was about 3 min.

After removing any remaining photoresist in an O_2 plasma etcher for 3 min, the SiN cantilevers on the front side of the wafer were released during wet etching [19] in a 20-wt% KOH solution at 75 °C. The etch time was around 4 h, which corresponded to a Si etch depth of around 200 μm. During etching, the back side of the wafer was protected by the continuous SiN film, for which the etch rate in KOH is essentially zero [19], [24], [25].

After the release, a typical 50-μm-long and 5-μm-wide cantilever was bent upward by about 800 nm as determined by optical profilometry. Previous investigations have shown [23] that the deposition of stoichiometric Si_3N_4 films by low-pressure CVD results in a substantially larger initial cantilever deflection. Therefore, we conclude that the Si-rich SiN films are characterized by a lower stress gradient in the z-direction than the stoichiometric films, which has initially motivated our choice for the former.

B. Film Deposition on Cantilevers

Amorphous $Ge_2Sb_2Te_5$ films were deposited on the SiN cantilevers using direct-current sputtering from a single target. To avoid oxidation and to obtain reproducible interface conditions, the $Ge_2Sb_2Te_5$ film was sandwiched between two thin layers of amorphous ZnS(80)–SiO_2(20), which were deposited using radio-frequency sputtering from a single target. ZnS(80)–SiO_2(20) was chosen because it is frequently used [26]–[31] as a capping layer in CD-RWs and DVDs. The sputtering background pressure was 7×10^{-7} mbar, and the working pressure during sputtering in Ar was 5×10^{-3} mbar. The Ar flow rate was 15 sccm. For $Ge_2Sb_2Te_5$, the sputtering power was 300 W, and the deposition rate was about 4.0 nm/s, which gave a film thickness of $h_f = 215 \pm 10$ nm. For ZnS(80)–SiO_2(20), the sputtering power was 1000 W, and the deposition rate was about 1.8 nm/s, which gave a film thickness of $h_{\mathrm{cap}} = 5 \pm 1$ nm for both layers. As determined from X-ray diffraction, the structure of the as-deposited $Ge_2Sb_2Te_5$ films was entirely amorphous, i.e., no evidence of partial crystallization during deposition was found.

The influence of the two ZnS(80)–SiO_2(20) layers on the cantilever curvature after crystallization of the $Ge_2Sb_2Te_5$ films is negligible. First, no phase transformation [31] occurs in the ZnS(80)–SiO_2(20). Second, the capping layers are so thin that they can be neglected in the calculations presented in Section II-A. This was verified analytically for the present conditions through the use of an equation based on (3) but extended to multilayers [14]. Therefore, in combination with the SiN thickness of $h_s = 211 \pm 3$ nm (Section III-A), the *experimental*

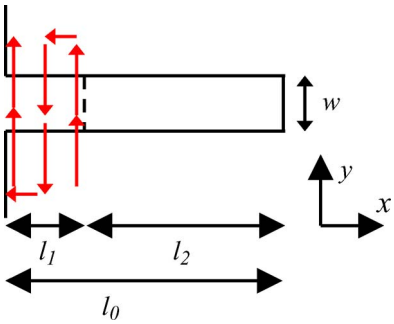

Fig. 7. Schematic top view of the cantilever shown in Fig. 1(b) during laser crystallization of a $Ge_2Sb_2Te_5$ film. The continuous laser beam is directed in the negative z-direction and remains on the optic axis of the lens. The movement of the sample stage is programmed so that the laser spot moves relative to the cantilever along the arrow. This method crystallizes $Ge_2Sb_2Te_5$ films on different cantilevers at the same power density, independent of length l_1.

thickness ratio is $h = h_f/h_s = 1.02 \pm 0.05$, which is close to the *desired* ideal value of $h_{\text{ideal}}^{(\text{SiN})} = 1.12$ reported in Section II-A. $p(h, m) = 0.58 \pm 0.03$ has been calculated using (4) from the *experimental* values, namely, $h = 1.02 \pm 0.05$ and $m^{(\text{SiN})} = M_f/M_s^{(\text{SiN})} = 0.15 \pm 0.03$ (Section II-A). The agreement of the experimental value $p(h, m) = 0.58 \pm 0.03$ with the *desired* maximum value $p_{\max}^{(\text{SiN})} = 0.58 \pm 0.04$ (Section II-A) is a result of the broad maximum in Fig. 5: Even though we were not quite able to manufacture cantilevers with the *desired* thickness ratio $h_{\text{ideal}} = 1.12$, our cantilevers are still expected to exhibit the maximum actuation angle α and maximum deflection δ.

C. Experimental Method

A laser diode (Shanghai Uniwave Technology, Model DPGL-2200, 532-nm wavelength, continuous operation, Gaussian beam profile, TEM_{00} mode) was coupled into an optical microscope using a beam splitter, which was aligned on the optic axis and focused on the sample through a 100× objective lens. The laser output power was adjustable up to a maximum of 250 mW. The computer-controlled sample stage could be moved laterally in two dimensions. A charge-coupled device camera was connected to the microscope, and the image of the sample was displayed on a monitor.

In order to laser-crystallize the region $l_1 \times w \times h_f$ of the amorphous $Ge_2Sb_2Te_5$ film (Fig. 1), the sample stage underneath the objective lens was moved perpendicular to the cantilever direction, while the cantilever was irradiated with the continuous laser beam (Fig. 7). The stage velocity was 0.1 mm/s, which is far slower than the velocity at which heat conduction in $Ge_2Sb_2Te_5$ and SiN occurs [32]. Due to the Gaussian beam profile, the temperature increases toward the middle of the laser beam. To ensure complete crystallization of the region $l_1 \times w \times h_f$, overlapping lines were crystallized. The associated reannealing of already crystallized regions does not affect the stress state of the film since stress relaxation in the *crystalline* phase occurs on a time scale of minutes to hours [10], [33]. This method allowed the consistent comparison of neighboring cantilevers of identical dimensions $l_0 \times w$ but different crystalline length l_1 since it leaves the laser spot size (and, therefore, the laser power density, i.e., the annealing temperature) constant. Crystallization was immediately observed on the monitor due to the pronounced increase in reflectivity [11], [34] and the movement of the free cantilever end to a position outside the focus plane of the lens [Fig. 9(a)]. Ablation could be detected as a reflectivity decrease in the center of the laser beam path. In order to find the ideal laser power that enables crystallization but avoids ablation, the power was decreased in small steps on different cantilevers until ablation no longer occurred in the laser beam center. This threshold power $(460 \pm 20\ \mu\text{W})$ was then used for the crystallization experiments. The power was measured with a conventional power meter underneath the objective lens at a laser spot diameter of about $1.6 \pm 0.2\ \mu$m (as measured from the width of a crystallized line). It is assumed that this threshold power is large enough to crystallize the film through its entire thickness h_f. A direct experimental verification of this assumption is difficult. However, an indirect justification was performed: Laser lines were crystallized into the continuous $Ge_2Sb_2Te_5$ film next to the cantilevers above the Si support. The threshold power was determined for this condition in a similar way. The depth of the surface dimple of these lines (which is a consequence of the volume contraction upon crystallization) was measured using an AFM (Digital Instruments 3100) and was found to be about 6.5%. This relative depth change agrees with literature values for laser-crystallized marks that extend through the entire film thickness of 85-nm-thick films [11], [34].

The cantilever height δ was measured both before and after laser crystallization (to incorporate in the analysis any initial deflection due to as-deposited stresses in SiN and/or $Ge_2Sb_2Te_5$). The height measurement was performed both through the focus setting of the optical microscope and using a noncontact profilometer (Veeco/Wyko NT2000).

D. Experimental Results

Fig. 8 shows a 50-μm-long and 5-μm-wide cantilever after deposition of amorphous $Ge_2Sb_2Te_5$ but before laser crystallization. The profilometer scan [Fig. 8(b) and (c)] reveals that the cantilever is bent downward to $\delta_0 = -1030 \pm 50$ nm at its free end. Since the SiN cantilever was bent upward by around 800 nm *before* the $Ge_2Sb_2Te_5$ deposition (determined by profilometry, not shown), the $Ge_2Sb_2Te_5$ as-deposited stress is slightly compressive. After laser crystallization along $l_1 = 4.6 \pm 0.5\ \mu$m (cf. Figs. 1 and 7), the cantilever is bent upward by $\delta^* = 7340 \pm 300$ nm (Fig. 9). Therefore, the laser-induced deflection change is $\delta = \delta^* - \delta_0 = 8370 \pm 350$ nm.

Fig. 10 shows a series of data points for different values of l_1. The cantilever deflection δ for those data points with $l_1 > 8\ \mu$m was measured using the focus knob of the optical microscope since the profilometer could not be used to measure the associated large angles. For $l_1 < 8\ \mu$m, δ was measured using the profilometer. The data were fitted to (2b), using $l_0 = 50\ \mu$m and r as a fit parameter. This results in $r = 27.8 \pm 0.9\ \mu$m. Using (3), this gives $\varepsilon_m = 1.31\% \pm 0.08\%$ for $h_s = 211 \pm 3$ nm and $p(h, m) = 0.58 \pm 0.03$. A fit to the data in Fig. 10 based on the exact expression for δ [(2a)] gives an almost identical fit curve and similar values: $r = 27.0 \pm 0.9\ \mu$m and

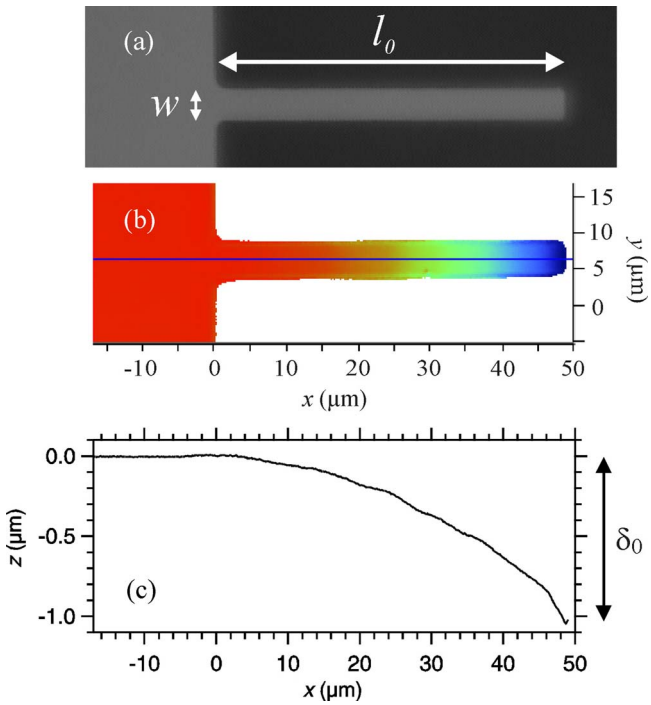

Fig. 8. SiN cantilever of 211 nm thickness onto which a 215-nm-thick amorphous $Ge_2Sb_2Te_5$ film has been deposited. The cantilever dimensions are $l_0 = 50$ μm and $w = 5$ μm (cf. Fig. 1). (a) (Top view) Optical micrograph. (b) (Top view) Profilometry scan. The colors represent height information (blue: low elevation; red: high elevation). (c) Profilometry scan, cross section along the line in (b). The cantilever is bent downward to $\delta_0 = -1030 \pm 50$ nm.

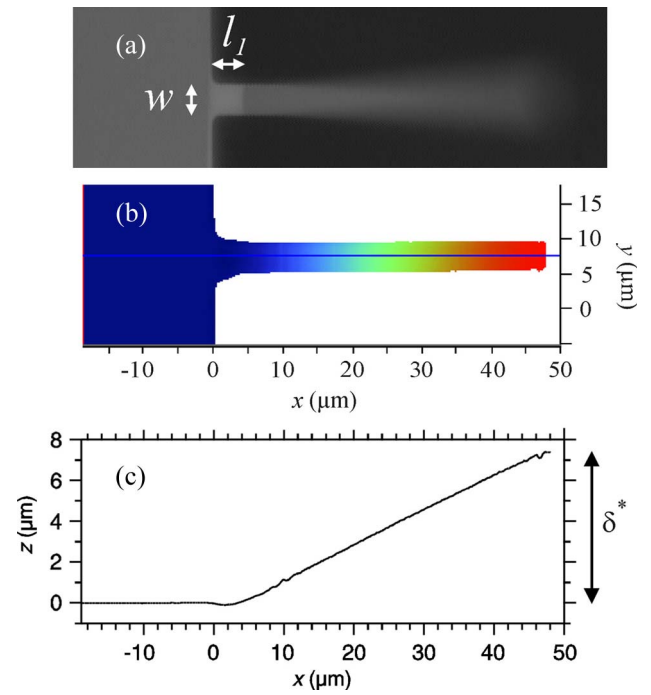

Fig. 9. Cantilever from Fig. 8 after laser crystallization along a length $l_1 = 4.6 \pm 0.5$ μm (cf. Figs. 1 and 7). (a) (Top view) Optical micrograph focused on the fixed cantilever end. The free cantilever end is outside the focal plane and is therefore not visible. The crystalline phase is characterized by a higher reflectivity than the amorphous phase. (b) (Top view) Profilometry scan. The colors represent height information (blue: low elevation; red: high elevation). (c) Profilometry scan, cross section along the line in (b). The cantilever is bent upward to $\delta^* = 7340 \pm 300$ nm.

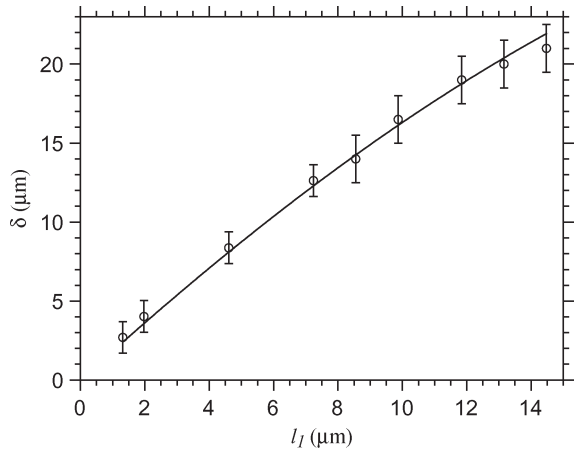

Fig. 10. Cantilever deflection δ at its free end as a function of the laser-crystallized length l_1. The cantilever dimensions are $l_0 = 50$ μm and $w = 5$ μm (cf. Figs. 1 and 6). The data are fitted with (2b), using the radius of curvature r as a fit parameter.

$\varepsilon_m = 1.35\% \pm 0.08\%$. This shows that the small-angle approximation [(2b)] holds. The elastically accommodated volume change upon laser crystallization is then $|\Delta V/V|_{\text{el}} = 3 \cdot \varepsilon_m = 4.05\% \pm 0.25\%$. This value does not yet account for the uncertainty in the deflection δ in the analytical model, which is estimated to be on the order of 5% for $l_1 > 2$ μm (cf. end of Section II-B). Since δ is proportional to ε_m [(6)], the corrected value is $|\Delta V/V|_{\text{el}} = 4.05\% \pm 0.45\%$, which takes into account this uncertainty.

We have also crystallized the amorphous $Ge_2Sb_2Te_5$ films on the SiN cantilevers in a furnace to check if the induced cantilever curvature is consistent with the laser-crystallization results. We used a crystallization temperature of 180 °C and a crystallization time of 1 min since it is known that annealing under these conditions leads to complete crystallization [8], [10], [35]–[38]. As a result, the radius of curvature of the furnace-crystallized cantilevers, as estimated directly from profilometer scans, is $r = 29 \pm 5$ μm. A more precise measurement was not possible due to the fact that the angle α was larger than 90°. Since this value for r agrees with the value found for laser crystallization, it can be concluded that the laser had crystallized the $Ge_2Sb_2Te_5$ film through its entire thickness, without significant ablation. In addition, it can be concluded that the laser transformed the film into its cubic (and *not* its hexagonal) crystal structure: Former studies have shown that furnace crystallization of amorphous $Ge_2Sb_2Te_5$ films at temperatures below about 310 °C results in the cubic structure, whereas furnace annealing above 310 °C gives the hexagonal structure [8]. The density of the hexagonal structure is 2% higher than that of the cubic structure [39], so that a potential laser crystallization into the hexagonal phase should give a substantially smaller radius of curvature compared with furnace crystallization into the cubic structure, which was not observed.

IV. Discussion

The elastically accommodated volume change, $|\Delta V/V|_{\text{el}} = 4.05\% \pm 0.45\%$, is significantly larger than expected from

available literature data: WC measurements [10] on 1000- and 85-nm-thick $Ge_2Sb_2Te_5$ films deposited on 200-μm-thick Si wafers have shown that a tensile film stress of about $\sigma_m^{(\mathrm{WC})} = 165 \pm 10$ MPa occurs upon crystallization (independent of the heating rate, which was between 0.1 and 20 K/min). Since the $Ge_2Sb_2Te_5$ film was much thinner than the Si wafer in the former study, both film stress $\sigma_m^{(\mathrm{WC})}$ and film strain $\varepsilon_m^{(\mathrm{WC})}$ are essentially constant along the direction normal to the wafer [14], [15]. Therefore, using $M_f = 45.2 \pm 8.2$ GPa, [17] the furnace-crystallization-induced elastic film strain in [10] is $\varepsilon_m^{(\mathrm{WC})} = \sigma_m^{(\mathrm{WC})}/M_f = 0.37\% \pm 0.07\%$, and the elastically accommodated volume change is $|\Delta V/V|_{\mathrm{el}}^{(\mathrm{WC})} = 3\varepsilon_m^{(\mathrm{WC})} = 1.10\% \pm 0.21\%$. This is almost four times smaller than the value of $|\Delta V/V|_{\mathrm{el}}$ measured in this paper. Therefore, the relatively stiff Si substrates in the WC study [10] are observed to induce more plastic stress relaxation in the $Ge_2Sb_2Te_5$ film than the much thinner and, therefore, much more flexible SiN cantilevers in this paper. Since the actuation angle α and height δ are proportional to $|\Delta V/V|_{\mathrm{el}}$ [(5) and (6)], this paper shows that phase-change materials are far more useful for applications in *externally* triggered microactuators or switches than it could be estimated *a priori* from available literature data.

The *total* volume change upon crystallization of *hypothetically* unconstrained $Ge_2Sb_2Te_5$ into the cubic crystal structure, $|\Delta V/V|_{\mathrm{tot}}$, was calculated [40] using $\varepsilon_m^{(\mathrm{WC})} = 0.37\% \pm 0.07\%$ and 6.5% $\pm$ 0.2% film thickness decrease as measured by X-ray reflectometry for the samples used in the WC study.[10] For this purpose, it was assumed that the total volume change is a sum of the elastically and inelastically accommodated volume changes. The result is $|\Delta V/V|_{\mathrm{tot}} = 6.92\% \pm 0.32\%$. Therefore, 59% $\pm$ 12% of the crystallization-induced volume change is accommodated elastically in this paper but only 16% $\pm$ 3% in the WC study [10].

It should be noted that any potential ablation during laser crystallization or any remaining amorphous regions would reduce the cantilever deflection δ. Since the analysis was based on the assumption that the laser crystallizes the $Ge_2Sb_2Te_5$ film through its entire thickness, the values of $\varepsilon_m = 1.35\% \pm 0.08\%$ and $|\Delta V/V|_{\mathrm{el}} = 4.05\% \pm 0.45\%$ would, in this case, serve as lower limits for the elastic mismatch strain and the elastically accommodated volume change, respectively.

The use of laser light to externally trigger the movement of microcantilevers was also investigated previously by Elliott *et al.* [41], [42]. Their studies show that thin films of amorphous AsSe alloys deposited on microcantilevers exhibit a reversible optomechanical effect: upon irradiating the films with laser light that is polarized parallel to the cantilever axis, an upward movement is observed, whereas perpendicularly polarized light induces a downward movement of the cantilever. Their effect however requires *continuous* laser irradiation: After switching off the laser power, the cantilever moves back to the original position irrespective of light polarization history. The cantilever in this paper, in contrast, remains displaced after cessation of laser illumination. Moreover, the magnitude of this displacement can be precisely controlled by the crystallized length l_1 (Fig. 10). This opens the door to new actuation applications.

An interesting follow-up project would be to investigate if the cantilever can be moved downward by reamorphizing the laser-crystallized $Ge_2Sb_2Te_5$. Under the assumption that the elastically accommodated volume changes upon laser-induced amorphization and laser-induced crystallization are identical, the actuator movement would then be reversible. Since $Ge_2Sb_2Te_5$ is a marginal glass former [33], [35], [43], crystallization can occur extremely fast. Therefore, very high cooling rates [32] on the order of 10^{10} K/s are necessary for successful amorphization: Laser-induced crystallization of $Ge_2Sb_2Te_5$ is possible [34], [44] with a pulsewidth of as short as 10 ns (at a laser power on the order of 5–10 mW), whereas laser-induced amorphization has been shown to be feasible [45] within a pulsewidth window of around 20–100 ns (at a power of at least 30 mW). Such a fast phase transformation could possibly allow the operation of an actuator that can be switched between two (or more) displacement states at a frequency of around $(100\ \mathrm{ns})^{-1} = 10$ MHz. This would be much faster than the effect in Elliott's studies, which proceeds on a time scale of seconds to be fully observed [41], [42]. We have not attempted the laser amorphization since we do not have access to a laser with the aforementioned short pulsewidth and high intensity. However, it should be noted that easier glass-forming materials which do not require such a high cooling rate for amorphization as $Ge_2Sb_2Te_5$ might be more useful for reversible actuation. $Ge_2Sb_2Te_5$ however exhibits the advantages of a large volume change and a fast phase transformation. Nevertheless, the fact that the cantilever is bent upward after crystallization (as opposed to flat) would complicate the laser focus regulation, which is necessary for a reproducible power density on the sample during amorphization.

V. Conclusions

1) If designed properly, thin microfabricated cantilevers coated with thin films offer a convenient method to measure film stresses or strains associated with laser-induced phase transformations: For any material combination in this bilayer configuration, an ideal film-to-cantilever thickness ratio exists that results in the largest possible cantilever deflection associated with the phase transformation in the film. This ideal thickness ratio depends *only* on the biaxial modulus ratio of the two layers. For $Ge_2Sb_2Te_5$ films on Si or SiN cantilevers, this thickness ratio is $h_{\mathrm{ideal}}^{(\mathrm{Si})} = 0.91 \pm 0.06$ and $h_{\mathrm{ideal}}^{(\mathrm{SiN})} = 1.12 \pm 0.09$, respectively. Moderate deviations from this ideal value still result in almost the same optimum cantilever deflection.
2) This method has been applied to measure the elastically accommodated volume change upon laser crystallization of 215-nm-thick $Ge_2Sb_2Te_5$ films deposited on 211-nm-thick SiN cantilevers. The result, $|\Delta V/V|_{\mathrm{el}} = 4.05\% \pm 0.45\%$, is almost four times larger than expected from previous wafer curvature measurements. Since the cantilever deflection is proportional to $|\Delta V/V|_{\mathrm{el}}$, this offers previously unknown potential for applications of these bilayers in externally triggered microactuators that can be stabilized in multiple positions.

ACKNOWLEDGMENT

The authors would like to thank M. Li and L. Shi (Data Storage Institute, Singapore) for depositing the $Ge_2Sb_2Te_5$ and ZnS(80)–SiO_2(20) films; P. S. Tierney, R. J. Bicchieri, R. A. Mönig, and A. R. Takahashi (Massachusetts Institute of Technology, Cambridge) for the useful discussions; and H. Yu and G. Zhou (National University of Singapore (NUS), Singapore) for their help with optical profilometry. In particular, Q. Guo would like to thank the Singapore–MIT Alliance for a graduate student fellowship.

REFERENCES

[1] N. Yamada, "Erasable phase-change optical materials," *MRS Bull.*, vol. 21, no. 9, pp. 48–50, Sep. 1996.

[2] E. R. Meinders, A. V. Mijiritskii, L. van Pieterson, and M. Wuttig, *Optical Data Storage: Phase-change media and recording*, ser. Philips Research Book Series, vol. 4. Dordrecht, The Netherlands: Springer-Verlag, 2006.

[3] C. A. Volkert and M. Wuttig, "Modeling of laser pulsed heating and quenching in optical data storage media," *J. Appl. Phys.*, vol. 86, no. 4, pp. 1808–1816, Aug. 1999.

[4] S. Hudgens and B. Johnson, "Overview of phase-change chalcogenide nonvolatile memory technology," *MRS Bull.*, vol. 29, no. 11, pp. 829–832, Nov. 2004.

[5] M. H. R. Lankhorst, B. W. S. M. M. Ketelaars, and R. A. M. Wolters, "Low-cost and nanoscale non-volatile memory concept for future silicon chips," *Nat. Mater.*, vol. 4, no. 4, pp. 347–352, Apr. 2005.

[6] Y. C. Chen, C. T. Rettner, S. Raoux, G. W. Burr, S. H. Chen, R. M. Shelby, M. Salinga, W. P. Risk, T. D. Happ, G. M. McClelland, M. Breitwisch, A. Schrott, J. B. Philipp, M. H. Lee, R. Cheek, T. Nirschl, M. Lamorey, C. F. Chen, E. Joseph, S. Zaidi, B. Yee, H. L. Lung, R. Bergmann, and C. Lam, "Ultra-thin phase-change bridge memory device using GeSb—IBM/Macronix/Qimonda joint project," in *IEDM Tech. Dig.*, San Francisco, CA, Dec. 11–13, 2006, pp. 1–4.

[7] D. Wamwangi, W. K. Njoroge, and M. Wuttig, "Crystallization kinetics of $Ge_4Sb_1Te_5$ films," *Thin Solid Films*, vol. 408, no. 1/2, pp. 310–315, Apr. 2002.

[8] I. Friedrich, V. Weidenhof, W. Njoroge, P. Franz, and M. Wuttig, "Structural transformations of $Ge_2Sb_2Te_5$ films studied by electrical resistance measurements," *J. Appl. Phys.*, vol. 87, no. 9, pp. 4130–4134, May 2000.

[9] W. K. Njoroge and M. Wuttig, "Crystallization kinetics of sputter-deposited amorphous AgInSbTe films," *J. Appl. Phys*, vol. 90, no. 8, pp. 3816–3821, Oct. 2001.

[10] T. P. Leervad Pedersen, J. Kalb, W. K. Njoroge, D. Wamwangi, M. Wuttig, and F. Spaepen, "Mechanical stresses upon crystallization in phase change materials," *Appl. Phys. Lett.*, vol. 79, no. 22, pp. 3597–3599, Nov. 2001.

[11] V. Weidenhof, I. Friedrich, S. Ziegler, and M. Wuttig, "Atomic force microscopy study of laser induced phase transitions in $Ge_2Sb_2Te_5$," *J. Appl. Phys.*, vol. 86, no. 10, pp. 5879–5887, Nov. 1999.

[12] R. Detemple, D. Wamwangi, M. Wuttig, and G. Bihlmayer, "Identification of Te alloys with suitable phase change characteristics," *Appl. Phys. Lett.*, vol. 83, no. 13, pp. 2572–2574, Sep. 2003.

[13] D. Wamwangi, R. Detemple, H.-W. Woeltgens, M. Wuttig, and X. Zhang, "Identifying Au-based Te alloys for optical data storage," *J. Appl. Phys.*, vol. 95, no. 12, pp. 7567–7572, Jun. 2004.

[14] L. B. Freund and S. Suresh, *Thin Film Materials—Stress, Defect Formation and Surface Evolution*. Cambridge, U.K.: Cambridge Univ. Press, 2003, pp. 86–127.

[15] L. B. Freund, J. A. Floro, and E. Chason, "Extensions of the Stoney formula for substrate curvature to configurations with thin substrates or large deformations," *Appl. Phys. Lett.*, vol. 74, no. 14, pp. 1987–1989, Apr. 1999.

[16] J. A. Kalb, Q. Guo, and C. V. Thompson, unpublished.

[17] J. Kalb, F. Spaepen, T. P. Leervad Pedersen, and M. Wuttig, "Viscosity and elastic constants of thin films of amorphous Te alloys used for optical data storage," *J. Appl. Phys.*, vol. 94, no. 8, pp. 4908–4912, Oct. 2003.

[18] W. A. Brantley, "Calculated elastic constants for stress problems associated with semiconductor devices," *J. Appl. Phys.*, vol. 44, no. 1, pp. 534–535, Jan. 1973.

[19] S. D. Senturia, *Microsystem Design*. Boston, MA: Kluwer, 2001, pp. 61–65. p. 187 and p. 196.

[20] H. Guo and A. Lal, "Die-level characterization of silicon-nitride membrane/silicon structures using resonant ultrasonic spectroscopy," *J. Microelectromech. Syst.*, vol. 12, no. 1, pp. 53–63, Feb. 2003.

[21] C. Serre, P. Gorostiza, A. Perez-Rodriguez, F. Sanz, and J. R. Morante, "Measurement of micromechanical properties of polysilicon microstructures with an atomic force microscope," *Sens. Actuators A, Phys.*, vol. 67, no. 1–3, pp. 215–219, May 1998.

[22] J. E. Sader, "Surface stress induced deflections of cantilever plates with applications to the atomic force microscope: Rectangular plates," *J. Appl. Phys.*, vol. 89, no. 5, pp. 2911–2921, Mar. 2001.

[23] R. J. Bicchieri, private communication.

[24] K. R. Williams and R. S. Muller, "Etch rates for micromachining processing," *J. Microelectromech. Syst.*, vol. 5, no. 4, pp. 256–269, Dec. 1996.

[25] K. R. Williams, K. Gupta, and M. Wasilik, "Etch rates for micromachining processing—Part II," *J. Microelectromech. Syst.*, vol. 12, no. 6, pp. 761–778, Dec. 2003.

[26] N. Ohshima, "Crystallization of germanium–antimony–tellurium amorphous thin film sandwiched between various dielectric protective films," *J. Appl. Phys.*, vol. 79, no. 11, pp. 8357–8363, Jun. 1996.

[27] N. Ohshima, "Structural analysis and crystallization studies of germanium–antimony–tellurium sputtered films on different underlayers," *J. Appl. Phys.*, vol. 83, no. 10, pp. 5244–5250, May 1998.

[28] E. R. Meinders, H. J. Borg, M. H. R. Lankhorst, J. Hellmig, and A. V. Mijiritskii, "Numerical simulation of mark formation in dual-stack phase-change recording," *J. Appl. Phys.*, vol. 91, no. 12, pp. 9794–9802, Jun. 2002.

[29] L. van Pieterson, M. van Schijndel, and J. C. N. Rijpers, "Te-free, Sb-based phase-change materials for high-speed rewritable optical recording," *Appl. Phys. Lett.*, vol. 83, no. 7, pp. 1373–1375, Aug. 2003.

[30] N. Nobukuni, M. Takashima, T. Ohno, and M. Horie, "Microstructural changes in GeSbTe film during repetitious overwriting in phase-change optical recording," *J. Appl. Phys.*, vol. 78, no. 12, pp. 6980–6988, Dec. 1995.

[31] W. K. Njoroge, H. Dieker, and M. Wuttig, "Influence of dielectric capping layers on the crystallization kinetics of $Ag_5In_6Sb_{59}Te_{30}$ films," *J. Appl. Phys.*, vol. 96, no. 5, pp. 2624–2627, Sep. 2004.

[32] J. A. Kalb, F. Spaepen, and M. Wuttig, "Kinetics of crystal nucleation in undercooled droplets of Sb- and Te-based alloys used for phase change recording," *J. Appl. Phys.*, vol. 98, no. 5, pp. 054 910/1–054 910/7, Sep. 2005.

[33] J. A. Kalb, "Stresses, viscous flow and crystallization kinetics in thin films of amorphous chalcogenides used for optical data storage," M.S thesis, RWTH Aachen Univ., Aachen, Germany, 2002.

[34] V. Weidenhof, I. Friedrich, S. Ziegler, and M. Wuttig, "Laser induced crystallization of amorphous $Ge_2Sb_2Te_5$ films," *J. Appl. Phys.*, vol. 89, no. 6, pp. 3168–3176, Mar. 2001.

[35] J. A. Kalb, M. Wuttig, and F. Spaepen, "Calorimetric measurements of structural relaxation and glass transition temperatures in sputtered films of amorphous Te alloys used for phase change recording," *J. Mater. Res.*, vol. 22, no. 3, pp. 748–754, Mar. 2007.

[36] N. Yamada, E. Ohno, K. Nishiuchi, N. Akahira, and M. Takao, "Rapid phase transitions of GeTe-Sb_2Te_3 pseudobinary amorphous thin films for an optical disk memory," *J. Appl. Phys.*, vol. 69, no. 5, pp. 2849–2856, Mar. 1991.

[37] J. Kalb, F. Spaepen, and M. Wuttig, "Atomic force microscopy measurements of crystal nucleation and growth rates in thin films of amorphous Te alloys," *Appl. Phys. Lett.*, vol. 84, no. 25, pp. 5240–5242, Jan. 2004.

[38] W. Welnic, J. A. Kalb, D. Wamwangi, C. Steimer, and M. Wuttig, "Outstanding meeting paper/review: Phase change materials—From structures to kinetics," *J. Mater. Res.*, vol. 22, no. 9, pp. 2368–2375, Sep. 2007.

[39] W. K. Njoroge, "Phase change optical recording—Preparation and X-ray characterization of GeSbTe and AgInSbTe films," Ph.D. dissertation, RWTH Aachen Univ., Aachen, Germany, 2001.

[40] U. Laudahn, S. Fähler, H. U. Krebs, A. Pundt, M. Bicker, U. v. Hülsen, U. Geyer, and R. Kirchheim, "Determination of elastic constants in thin films using hydrogen loading," *Appl. Phys. Lett.*, vol. 74, no. 5, pp. 647–649, Feb. 1999.

[41] P. Krecmer, A. M. Moulin, R. J. Stephenson, T. Rayment, M. E. Welland, and S. R. Elliott, "Reversible nanocontraction and dilatation in a solid induced by polarized light," *Science*, vol. 277, no. 5333, pp. 1799–1802, Sep. 1997.

[42] M. Stuchlik and S. R. Elliott, "All-optical actuation of amorphous chalcogenide-coated cantilevers," *J. Non-Cryst. Solids*, vol. 353, no. 3, pp. 250–262, Mar. 2007.

[43] J. Kalb, F. Spaepen, and M. Wuttig, "Calorimetric measurements of phase transformations in thin films of amorphous Te alloys used for optical data storage," *J. Appl. Phys.*, vol. 93, no. 5, pp. 2389–2393, Mar. 2003.
[44] J. H. Coombs, A. P. J. M. Jongenelis, W. van Es-Spiekman, and B. A. J. Jacobs, "Laser-induced crystallization phenomena in GeTe-based alloys. II. Composition dependence of nucleation and growth," *J. Appl. Phys.*, vol. 78, no. 8, pp. 4918–4928, Oct. 1995.
[45] V. Weidenhof, N. Pirch, I. Friedrich, S. Ziegler, and M. Wuttig, "Minimum time for laser induced amorphization of $Ge_2Sb_2Te_5$ films," *J. Appl. Phys.*, vol. 88, no. 2, pp. 657–664, Jul. 2000.

Johannes A. Kalb received the M.S. and Ph.D. degrees in physics (with highest honors) from the Technical University of Aachen (RWTH), Aachen, Germany, in 2002 and 2006, respectively. His M.S. and Ph.D. research work focused on stresses and crystallization kinetics in phase-change materials.

During his graduate studies in 2001, 2003, and 2004, he conducted research at the School of Engineering and Applied Sciences, Harvard University, Cambridge, MA. Since 2006, he has been with the Department of Materials Science and Engineering, Massachusetts Institute of Technology (MIT), Cambridge, as a Postdoctoral Researcher. After a research assignment at the National University of Singapore, Singapore, in the summer of 2007 as part of the Singapore–MIT Alliance, he joined Intel Corporation, Santa Clara, CA, in the fall of 2007, to continue research on phase-change materials.

Dr. Kalb received the Friedrich-Wilhelm Award of RWTH Aachen for his M.S. thesis. He was granted research fellowships from the Studienstiftung des Deutschen Volkes (2003–2006) and the Alexander von Humboldt Foundation (2006–2007).

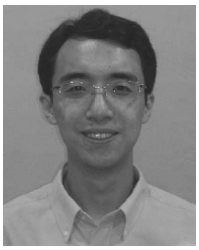

Qiang Guo received the B.S. degree in microelectronics from Peking University, Beijing, China, in 2005, and the M.Eng. degree in materials science and engineering from the Massachusetts Institute of Technology (MIT), Cambridge, in 2006. He is currently working toward the Ph.D. degree in the Program for Advanced Materials for Micro- and Nano-Systems, Singapore–MIT Alliance, National University of Singapore (NUS), Singapore, under the supervision of Prof. Y. Li (NUS) and Prof. C. Thompson (MIT).

His research includes the applications of phase-change materials and amorphous metals in micro- and nanosystems.

Xiaoqiang Zhang received the B.Eng. degree in materials engineering from Shenyang University of Technology, Shenyang, China, in 1997, and the M.E. and Ph.D. degrees in material science and engineering from the Institute of Metal Research, Chinese Academy of Sciences, Beijing, China, in 2000 and 2005, respectively.

He was a Research Fellow with the Singapore–MIT Alliance, National University of Singapore (NUS), Singapore, from 2005 to 2007. He joined Chartered Semiconductor Manufacturing Ltd., Singapore, at the end of 2007. His research interests include precise engineering, MEMS, and nanotechnology. He has authored or coauthored 13 publications and is the holder of three patents.

Yi Li received the B.E. degree from Huazhong University of Science and Technology, Wuhan, China, and the Ph.D. degree from the University of Sheffield, Sheffield, U.K.

He is an Associate Professor with the Department of Materials Science and Engineering, National University of Singapore (NUS), Singapore. Following a three-year postdoctoral research appointment at the University of Sheffield, he joined NUS in 1992. His current research work includes bulk metallic amorphous materials, glass formation, and mechanical and thermal properties of bulk metallic glasses for both functional and structural applications.

Chornghaur Sow received the B.Sc. (first-class honors) and M.S. degrees in physics from the National University of Singapore (NUS), Singapore, in 1991 and 1993, respectively, and the Ph.D. degree from the University of Chicago, Chicago, IL, in 1998.

During 1999–2000, he was a Postdoctoral Fellow with Bell Labs, Lucent Technologies. He has been with the Department of Physics, Faculty of Science, NUS, since 2001, where he is currently an Associate Professor. He has authored or coauthored a number of papers in the field of nanoscience and nanomaterials.

Dr. Sow is a member of the NUS Nanoscience and Nanotechnology Initiative.

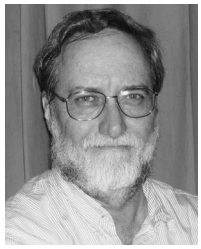

Carl V. Thompson received the S.B. degree in materials science and engineering from the Massachusetts Institute of Technology (MIT), Cambridge, and the S.M. and Ph.D. degrees in applied physics from Harvard University, Cambridge, MA, the latter in 1981.

He is the Stavros Salapatas Professor of Materials Science and Engineering with the Department of Materials Science and Engineering, MIT. He is currently the MIT Cochair of the Program for Advanced Materials for Micro- and Nano-Systems, Singapore–MIT Alliance, Singapore, and is the Director of the Materials Processing Center, MIT. His research includes processing of thin films and nanostructures for use in electronic and electromechanical devices and systems.

Dr. Thompson was awarded a U.K. SERC Fellowship for research in the Department of Metallurgy and Materials Science, Cambridge University, Cambridge, U.K., during the 1990–1991 academic year. He received an Alexander von Humboldt Research Award for Senior U.S. Scientists and carried out research at the Max-Planck-Institut für Metallforschung, Stuttgart, Germany, during the 1997–1998 academic year. He served as the President of the Materials Research Society in 1996.